

USER GUIDE

CYMA2DV: Non-LTE radiative transfer in cylindrical threads with incident radiation (2D transfer with 3D velocity fields)

Martine Chane-Yook

`martine.chane-yook@universite-paris-saclay.fr`

Reviewed by:

Jean-Claude Vial
Pierre Gouttebroze
Jacques Dubau

Web access:

<https://idoc.osups.universite-paris-saclay.fr/medoc/tools/radiative-transfer-codes/>

Contents

1	Introduction	2
2	Description of CYMA2DV code	2
3	Algorithm	3
4	Cylindrical thread modeling	5
5	Bound-Free and Bound-Bound transitions	9
6	Hydrogen atomic structure	9
7	Population equations and radiative transfer equation	10
8	Formalism used for radiative transfer	12
9	Subroutine descriptions	13
9.1	Set of variables used in HYCY2D subroutine	14
9.2	Hydrogen modeling (Johnson model, [19])	15
10	Results for hydrogen lines in cylindrical threads	20
11	Running CYMA2DV	27
12	CPU time	28
13	Acknowledgements	28
	Bibliography	29

1 Introduction

The CYMA2DV code was written in Fortran 77 by P. Gouttebroze ([12], [11]) and describes Non-LTE (NLTE) radiative transfer (2D) for hydrogen atom in a cylindrical thread inside the solar corona, with incident radiation including 3D gas velocity fields, using complete frequency redistribution. We solve simultaneously the equations of NLTE radiative transfer, statistical equilibrium of hydrogen level populations, and electric neutrality. To solve the present problem, it is convenient to use cylindrical and cartesian coordinates in parallel.

This code is more general than for large prominences since it treats multi-dimensionnal radiative transfer in chromospheric and coronal loops.

These hydrogen lines (intensity, profiles) are used to diagnose solar prominences through comparison with observations.

Two types of atmosphere models are considered here:

- model whose parameters don't vary inside the cylinder, defined by DIAM, TMOD, PG-MOD, ALDEG, HAL (cylinder diameter (km), temperature ($^{\circ}\text{K}$), gas pressure (dyn.cm^{-2}), angle of inclination of the cylinder (in degree), altitude (km))
- model whose parameters vary inside the cylinder, defined by PGMOD, ALDEG, HAL, R0KM, R1KM, T0, T1 (gas pressure (dyn.cm^{-2}), angle of inclination of the cylinder (in degree), altitude (km), internal radius (km), external radius (km), temperature ($^{\circ}\text{K}$) inside R0KM, temperature between R0KM and R1KM).

The original version of CYMA2DV, adapted to **gfortran** compiler is available from MEDOC website:

<https://idoc.osups.universite-paris-saclay.fr/medoc/tools/radiative-transfer-codes/>

In the following sections, we will explain in details CYMA2DV code (hydrogen): modeling, implemented equations, algorithm, numerical methods, etc.

2 Description of CYMA2DV code

Nature of the physical problem: NLTE radiative transfer (2D) in a cylinder with incident radiation and 3D velocity fields (*HI*, *II* lines)

Method of solution: Λ -iteration method + preconditioning (MALI)

Other relevant information: * Two types of models:

- model whose parameters don't vary inside the cylinder, defined by DIAM, TMOD, PG-MOD, ALDEG, HAL (cylinder diameter (km), temperature ($^{\circ}\text{K}$), gas pressure (dyn.cm^{-2}), angle of inclination of the cylinder (in degree), altitude (km))
- model whose parameters vary inside the cylinder, defined by PGMOD, ALDEG, HAL, R0KM, R1KM, T0, T1 (gas pressure (dyn.cm^{-2}), angle of inclination of the cylinder (in degree), altitude (km), internal radius (km), external radius (km), temperature ($^{\circ}\text{K}$) inside

R0KM, temperature between R0KM and R1KM).

* Complete frequency redistribution (CRD) is used for hydrogen lines and continua

Author: P. Gouttebroze

Program available from:

<https://idoc.osups.universite-paris-saclay.fr/medoc/tools/radiative-transfer-codes/>

Computer(s) on which program has been tested: PC with 4 Intel processors (2.67GHz)

Operating System(s) for which version of program has been tested: Linux

Programming language used: Adapted in Fortran 90 for **gfortran** compiler

Status: Stable

Accessibility: open (MEDOC)

No. of code lines in combined program and test deck: cyma2dv.f90 (~ 3000 lines), visu.f90 (~ 2000 lines)

Typical running time: 1h18 for a given model whose parameters vary inside the cylinder

References:

- P. Gouttebroze, “Radiative transfer in cylindrical threads with incident radiation. V : 2D transfer with 3D velocity fields”, A&A 487, 805-813, 2008
- P. Gouttebroze, “Radiative transfer in cylindrical threads with incident radiation. III : Hydrogen spectrum”, A&A, 448, 367-374, 2006

3 Algorithm

The figure 1 describes the algorithm of CYMA2DV code.

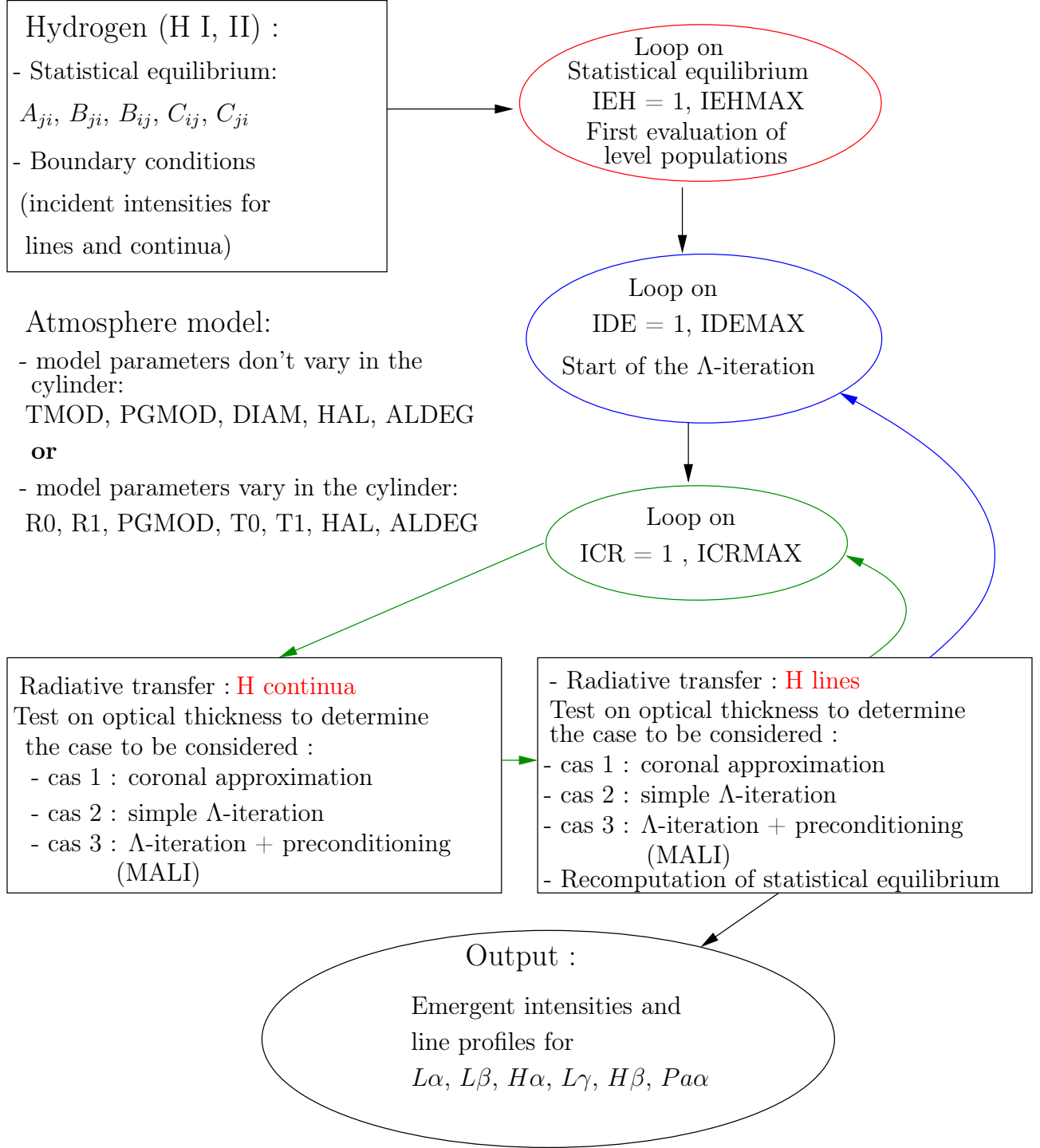


Figure 1: Algorithm of CYMA2DV code

4 Cylindrical thread modeling

To solve the present problem, it is convenient to use cylindrical and cartesian coordinates in parallel.

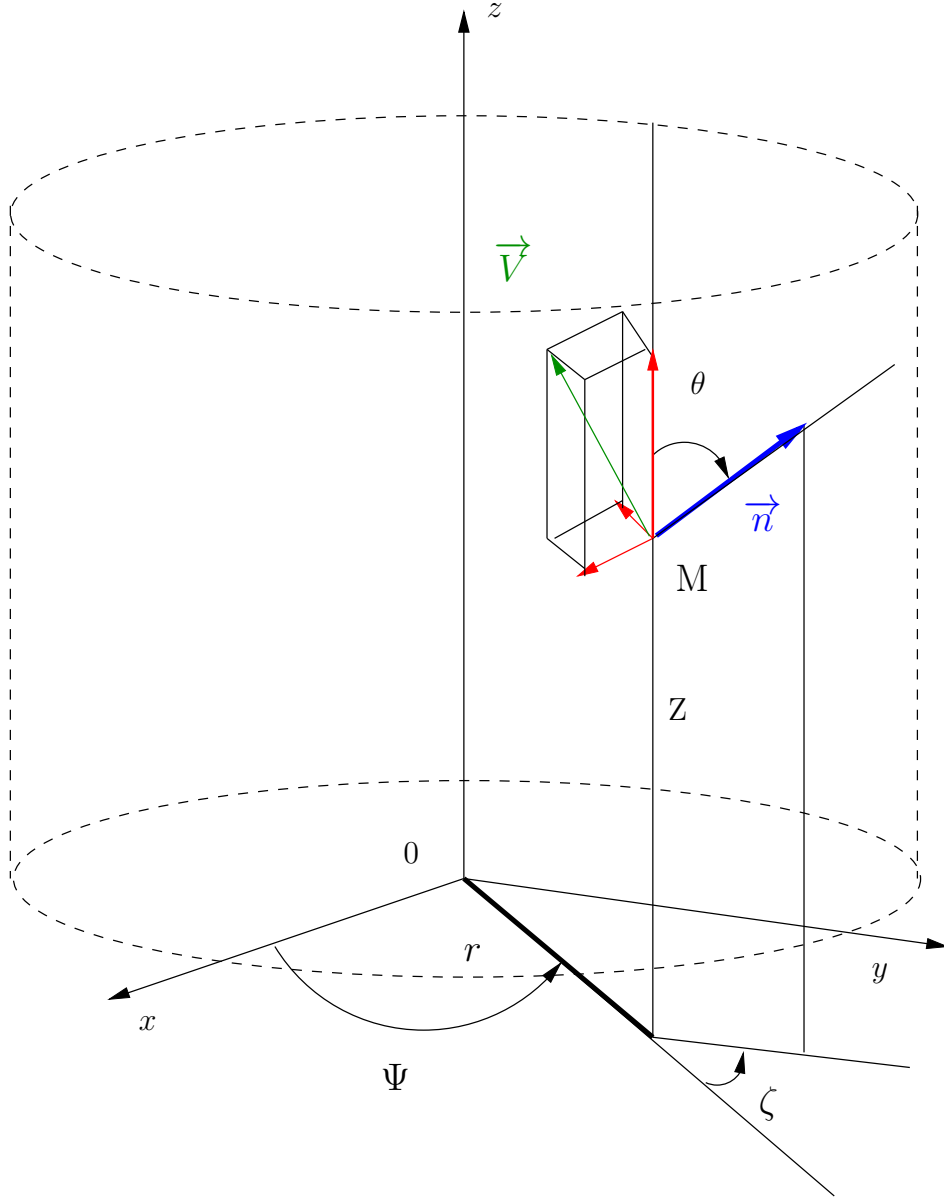


Figure 2: Coordinate system for a cylinder

Figure 2 represents coordinate system used for the cylinder with axis z . To describe this cylinder, a cylindrical meshing is done for the core (e.g. 6 cylindrical meshes) up to internal

radius R0KM and for the transition region up to R1KM (e.g. 6 cylindrical meshes). These meshes are divided in NR submeshs to solve the radiative transfer.

The running point M is defined by 3 cylindrical coordinates (r, Ψ, z) or alternatively by 3 cartesian coordinates $(x = r \cos \Psi, y = r \sin \Psi, z)$.

The direction of a ray at point M is defined by the vector \mathbf{n} corresponding to angles (ζ, θ) , $\zeta \in [-\pi, \pi]$ and $\theta \in [0, \pi]$. ζ is in the (x, o, y) plan and θ is the angle between \mathbf{n} and z-axis. The gas velocity is defined by the vector \mathbf{V} , which is function of (r, Ψ) . The third (longitudinal) component V_z is the same for the cartesian and cylindrical coordinates. The two first componants are written as:

$$\begin{aligned} V_x &= V_r \cos \Psi - V_\Psi \sin \Psi \\ V_y &= V_r \sin \Psi - V_\Psi \cos \Psi \end{aligned} \tag{4.1}$$

Figure 3 shows the inclination angle α (in degree) of the cylinder, angle between cylinder axis and the vertical with respect to the solar surface. In figure 3, $\alpha = 90$. Figure 4 also illustrates this inclination angle α . The cylinder is considered as infinite in length.

The aim of CYMA2DV code is to treat the radiative transfer inside a cylinder in two-dimensions. 2D codes ([12], [15]) are generally used for loop modelings ([11]) and not to treat large prominences. Figure 4 is an example of semi-toric loop. More precisely, different models (of cylinder) can be put together to build a loop model ([11]).

In paragraph 10 (hydrogen results), the cylinder model considered is the cylinder which is at the bottom of the semi-toric loop (vertical cylinder, ALDEG = 0° , altitude HAL = 0 km in the input file “paramod.dat”) in figure 4.

Figure 5 represents the trajectory of a photon inside the cylinder in the transversal plan. For this example, there are 6 points in the r -grid ($s_1, s_2, s_3, s_4, s_5, s_6, \dots$).

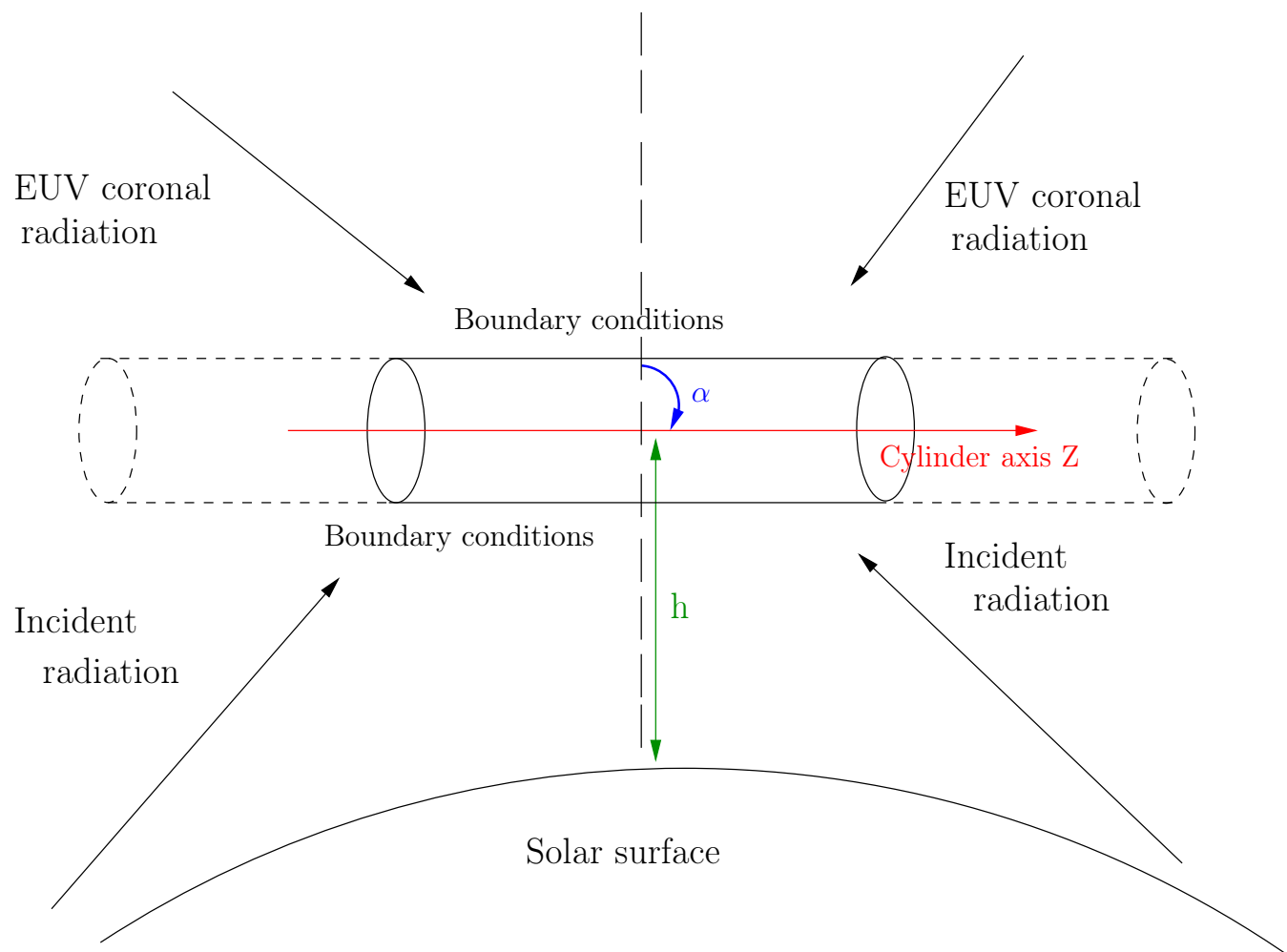


Figure 3: Infinite cylinder model

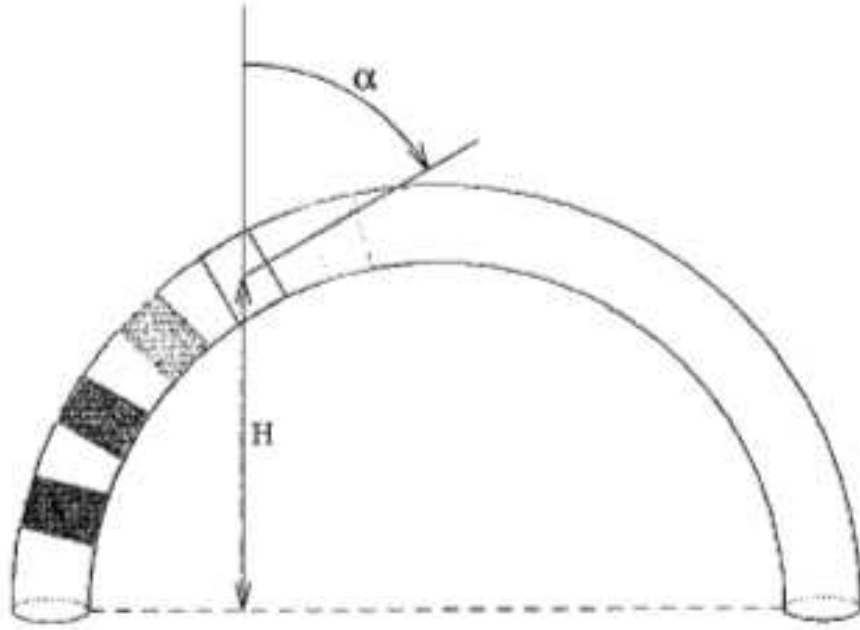


Figure 4: Semi-toric loop

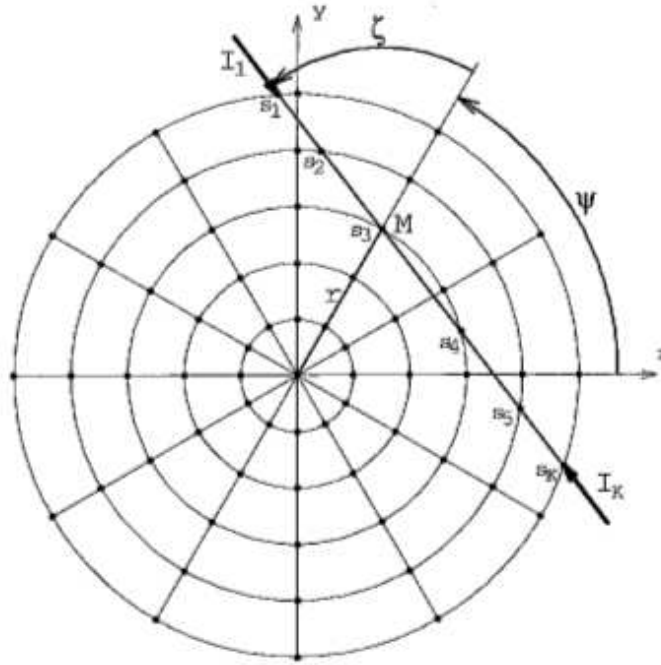


Figure 5: Trajectory of a photon inside the cylinder

5 Bound-Free and Bound-Bound transitions

The transitions used in CYMA2DV code are Bound-Free and Bound-Bound transitions, which are represented in figure 6. Bound-Free transitions are between a bound state i and a continuum, producing a free electron with energy ϵ . It starts from excited states limit, i.e. $\epsilon = 0$. Bound-Bound transitions are from level i to level j .

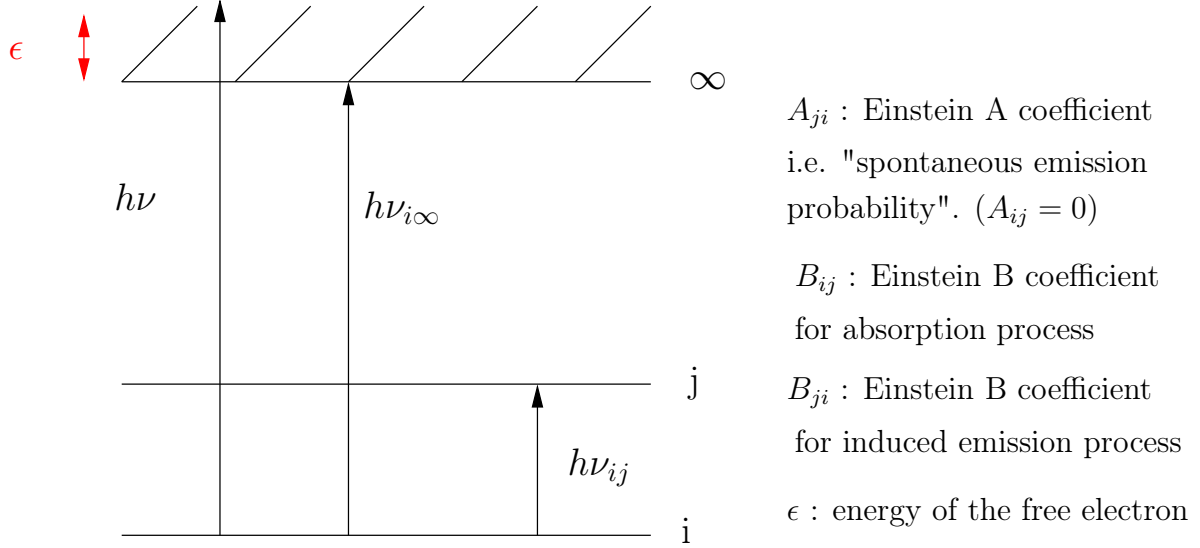


Figure 6: Transition types used in CYMA2DV

6 Hydrogen atomic structure

The transitions for hydrogen are summarized in Table 1. NN is the number of energy levels, including the threshold level continuum, bound levels limit (∞). $NTT = NN \times (NN - 1)/2$ is the total number of transitions, $NTRC = NN - 1$ is the number of continua (bound-free transitions) and $NTAR = NTT - NTAC$ is the number of lines (bound-bound transitions). In CYMA2DV, $NN = 6$ (5 levels and 1 continuum).

Transition	Lower level	Upper level	Transition name	Wavelength $\lambda(\text{\AA})$
1	1	2	$Ly - \alpha$	1215
2	1	3	$Ly - \beta$	1025
3	2	3	$H - \alpha$	6564
4	1	4	$Ly - \gamma$	972
5	2	4	$H - \beta$	4862
6	3	4	$Pa - \alpha$	18756
7	1	5	$Ly - \delta$	949
8	2	5	$H - \gamma$	4341
9	3	5	$Pa - \beta$	12821
10	4	5	$Br - \alpha$	6563
11	1	6	$Ly - \epsilon$	973
12	2	6	$H - \delta$	4102
13	3	6	$Pa - \gamma$	10935
14	4	6	$Br - \beta$	4861
15	5	6	$Pf - \alpha$	7460
16	1	7	$Ly - 6$	931
17	2	7	$H - \epsilon$	3971
...
$NTAR + 1$	1	NN	Lyman Continu	911
$NTAR + 2$	2	NN	Balmer continu	3645
...
$NTT =$	$NN - 1$	NN		

Table 1: Main transitions for hydrogen

7 Population equations and radiative transfer equation

Let's consider level j in figure 6. At equilibrium, the population equations for this level contain all processes of population and depopulation of level j to other levels i which are balanced:

$$N_j \sum_{j \neq i}^n P_{ji} = \sum_{j \neq i}^n N_i P_{ij} \quad (7.1)$$

The depopulation rate P_{ji} from level j is written as :

$$P_{ji} = A_{ji} + B_{ji} \bar{J}_{ij} + C_{ji} = R_{ji} + C_{ji} \quad (7.2)$$

where C_{ji} is the collisional deexcitation rate, proportional to the electron density. R_{ji} is the radiative depopulation probability either by absorption and by spontaneous (A_{ji}) or by stimulated emission. A_{ji} and B_{ji} are corresponding to Einstein coefficients.

The population rate P_{ij} of level j can also be written as :

$$P_{ij} = B_{ij} \bar{J}_{ij} + C_{ij} = R_{ij} + C_{ij},$$

where R_{ij} and C_{ij} are similar to R_{ji} and C_{ji} , except for spontaneous emission ($A_{ij} = 0$). The left-hand side term in the population equations (7.1) represents all the processes which depopulate level j and the right-hand side term corresponds to all the levels which populate the level j . And we use the following closure conservation equation:

$$\sum_{j=1}^n N_j = N_T \quad (7.3)$$

where N_T is the total population of the atomic element.

These population equations (7.1) which contain the mean intensities via \bar{J}_{ij} (7.9) are coupled with the radiative transfer equation (7.4).

The specific intensity I in the radiative transition is obtained by solving the transfer equation:

$$\frac{dI(\Delta\nu, \mathbf{n})}{ds} = k_{ij}(\Delta\nu, \mathbf{n})[S_{ij} - I(\Delta\nu, \mathbf{n})], \quad (7.4)$$

s is the abscissa along the ray, \mathbf{n} is the direction of the ray, $\Delta\nu$ is the frequency difference with the frequency line center ν_{ji} , S_{ij} is the source function (independent of frequency and direction, under the assumption of complete redistribution) :

$$S_{ij} = \frac{N_j A_{ji}}{N_i B_{ij} - N_j B_{ji}} \quad (7.5)$$

$k_{ij}(\Delta\nu, \mathbf{n})$ is the absorption coefficient in a spectral line:

$$k_{ij}(\Delta\nu, \mathbf{n}) = k_{ij}^M \phi(\Delta\nu, \mathbf{n}), \quad (7.6)$$

with

$$k_{ij}^M = \frac{h \nu_{ji}}{4\pi} (N_i B_{ij} - N_j B_{ji}) \quad (7.7)$$

ϕ is the normalized absorption profile (which is also the emission profile under the assumption of complete redistribution):

$$\phi(\Delta\nu, \mathbf{n}) = \frac{1}{\sqrt{\pi}\Delta\nu_D} H \left[a, \frac{1}{\Delta\nu_D} \left(\Delta\nu - \frac{\nu_{ji}}{c} \mathbf{n} \cdot \mathbf{V} \right) \right], \quad (7.8)$$

where H is the Voigt function, c is the speed of light, $\Delta\nu_D$ the Doppler width, a the damping factor (natural broadening + collisional broadening + ...), \mathbf{V} is the velocity vector of the gas.

The mean intensity \bar{J}_{ij} is obtained by integrating the specific intensity, multiplied by the absorption profile, with respect to frequency and direction:

$$\bar{J}_{ij} = \frac{1}{4\pi} \int_{-\infty}^{+\infty} d(\Delta\nu) \oint I(\Delta\nu, \mathbf{n}) \phi(\Delta\nu, \mathbf{n}) d\Omega, \quad (7.9)$$

where Ω is the solid angle.

Thus, we obtain a coupled equation system which is solved by numerical methods such as accelerated Lambda-Iteration method (MALI, [24], [22]). For more details, see the next two sections.

8 Formalism used for radiative transfer

We start with an initialization of level populations, radiation field, electron density, atomic parameters (Einstein A and B coefficients, collision rate coefficients), input model, incident intensities for lines and continua, boundary conditions. Iterative processes can now begin:

- The first loop on IEH , independant of the other loops, concerns the computation of statistical equilibrium by assuming that the medium is optically thin for all transitions (i.e. without radiative transfer).
- The second loop on IDE (beginning of the Λ -iteration), including an internal loop (on ICR), concerns radiative transfer for bound-free and discrete transitions. This loop (on IDE) finishes with a test convergence. New radiative parameters (P_{ji}) are calculated.

The statistical equilibrium (7.1, 7.3) consists of the solution of a linear system (by elimination methods) whose terms are obtained from population and depopulation coefficients P_{ji} (7.2). The unknowns are level populations.

The radiative transfer (7.4) consists in computing intensities in spectral lines or continua from the knowledge of the source function (7.5) and the intensities (boundary conditions). We use the Λ -iterative method ([27], [24]): numerical method of a linear system leading to a tridiagonal matrix. We consider 3 cases:

- optical thin case: we use the coronal approximation
- simple Λ -iterative method
- Λ -iterative method with preconditioning (MALI, [24], [22]).

The simple Λ -iterative method consists in introducing an operator Λ in the formula of the source function by omitting the dependence with optical depth. It is well-known that this method is very slow to converge since optical thickness becomes significant. To accelerate the simple Λ -iterative method we use the MALI method which consists in choosing for the approximate operator Λ^* the exact diagonal of the complete operator Λ .

In output, we obtain the mean intensity (7.9) from which new source functions (7.5) and new transition rates can be computed. Source functions will be used later for the computation of emergent intensities and line profiles.

For lines and continua, we use complete frequency redistribution which supposes that there is no relation between frequency of the absorbed photon and frequency of reemitted photon. In the present problem, we neglect continuum absorption.

9 Subroutine descriptions

CYMA2DV starts by reading atmosphere parameters (“paramod.dat”) and mesh parameters. The main subroutine **HYCY2D** is then called.

Input files for CYMA2DV:

- intinc.dat: incident intensities for the main hydrogen lines
- tembri.dat: other lines of the hydrogen spectrum (Brightness temperatures)
- paramod.dat: model to be considered, defined by the following parameters:
DIAM, TMOD, PGMOD, ALDEG, HAL, R0KM, R1KM, T0, T1, TREF (cylinder diameter (km), temperature (°K), gas pressure (dyn.cm^{-2}), inclination angle of the cylinder (in degree), altitude (km), internal radius (km), external radius (km), temperature inside the internal radius (°K), temperature between R0KM and R1KM (°K), reference temperature (°K)).

Two types of models:

- ★ If ITVAR=0: model whose parameters don’t vary inside the cylinder, defined by ALDEG, HAL, DIAM, TMOD, PGMOD
- ★ If ITVAR=1, model whose parameters vary inside the cylinder, defined by ALDEG, HAL, R0KM, R1KM, T0, T1, PGMOD, TREF. The other unused variables are set to zero.

Output files for CYMA2DV:

- resu2dv.dat: file containing emergent intensities. It is the input data of the visualization program “visu.f90”. Output: cosbovi.ps (hydrogene line profiles)
- popc2dv.dat: hydrogen level populations
- cc2dhv.log: iteration message
- fort.8: CPU time

In the next sections, hydrogen modeling will be explained in details, such as all subroutines called by CYMA2DV code and a set of variables used in HYCY2D subroutine.

9.1 Set of variables used in HYCY2D subroutine

- ITVAR = 0: model whose parameters don't vary inside the cylinder, ITVAR = 1: model whose parameters vary inside cylinder
- NPSI: number of points for the angular variable PSI (Ψ)
- RR (array of size NR): radius of successive layers from the center
- TAU: optical thickness (between two points)
- NZETA: number of polar coordinates ζ
- NTHET: number of polar coordinates θ
- NFR: number of frequencies in a line
- NTAB: size of the temperature array TAB (for the computation of collision rate coefficients)
- NINF: transition lower level
- NSUP: transition upper level
- AJI: Einstein A coefficient i.e. spontaneous emission
- BJI, BIJ: Einstein B coefficients for absorption and induced emission processes
- CIJ, CJI: collisional excitation/deexcitation coefficients
- CPOL: polynomial coefficients of degree 5 used in the computations of dilution factors (array size : NCMX)
- RIJ, RJI: radiative transition rates
- FRR: frequency in the line
- Atmospheric parameters (array of size $NPSI \times NR$): TE (temperature), PG (gas pressure), VT (microturbulent velocity), HNH (hydrogen density: number of atoms per unit volume), HNE (electron density)
- HN: hydrogen level populations
- FRN: level frequency
- XFR and XFRC: division models in frequency for lines and continua
- PHIL: absorption profile
- SF: source function

- CAFR: absorption coefficient
- ITRC and ITRD: control index for lines and continua
- OIS: collisional ionization rate coefficient

9.2 Hydrogen modeling (Johnson model, [19])

Hydrogen modeling (HYCY2D subroutine) is divided in several parts:

- Initialization of level populations ($HN = 0$).
- MATIPS: computation of interpolation matrix in Ψ (PSI in the subroutine). The points are not necessarily on a node of the grid or inside the grid.
- Definition of the frequency grid XFR which is the same for all lines
- Definition of grids in ζ (ZETA in the subroutine) and in θ (THETA in the subroutine)
- Definition of lower levels, upper levels and control index for hydrogen
- Definition of hydrogen energy levels
- Division in frequency for lines and continua
- Computation of spontaneous emission probabilities
- Computation of broadening constants
- Computation of collisional excitation and ionization coefficients *OIS* using *TAB*
- Computation of incident intensities for lines:
 - ★ SOLINH: preparation of boundary conditions
 - ★ CIIM2: computation of mean incident intensities
- computation of incident intensities for continua from the input file “tembri.dat”
 - ★ CIIM2: computation of mean incident intensities
- Computation of mean intensities for lines in the optically thin case and RIJ coefficients
- *do IEH = 1, IEHMAX*: loop on statistical equilibrium
 - ★ update of level populations and initialization of electron density $N_e = 1/2 N_H$
 - ★ TXCH2D: computation of collisional transition rates
 - ★ Computation of radiative transition rates in bound-free transitions
 - ★ EQST2D: computation of level populations

- enddo (*IEH*)
- Beginning of Λ -iteration
- Initialization of trajectories with computation at each point of abscissa and Doppler shifts due to velocity field
- DEFCV: definition of velocity field
- *do IDE = 1, IDEMAX*: loop on Λ -iteration
 - ★ *do ICR = 1, ICRMAX*: internal loop
 - Radiative transfer for discrete transitions:
 - ▷ Computation of source functions and optical thicknesses to determine the method to be used (case 1, case 2 or case 3):
 - ▷ Case 1: coronal approximation
 - ▷ Case 2: simple Λ -iteration method
 - . STYC2D: computation of intensity along a ray crossing the cylinder, knowing absorption coefficients (7.6), source functions (7.5) and incident intensities at each extremity of the cylinder
 - ▷ Case 3: Λ -iteration + preconditioning (MALI)
 - . STYC2D
 - . DZTC2DV: computation of the contribution to the diagonal of the Λ operator for a cylinder, knowing the absorption coefficient along the trajectory
 - Radiative transfer for bound-free transitions: same process as for discrete transitions (STJC2D: equivalent to STYC2D for continua)
 - EQST2D: statistical equilibrium
 - ★ enddo (*ICR*)
 - ★ Convergence test
- Prints quantities in output files

Subroutines called before are explained in the next paragraph.

Computation of collisional excitation and ionization rate coefficients OIS, of spontaneous emission probabilities AJI, BJI, BIJ

Computation of hydrogen atomic parameters for statistical equilibrium: Einstein A and B coefficients for photons (AJI , BIJ , BJI : independent of electron temperature), collisional excitation and ionization rate coefficients (OIS in CYMA2DV code) for electrons, called S_e and S_i in the formulas below. These coefficients are independent of electron temperature.

The model used for hydrogen is L.C. Johnson model ([19]).

AJI is obtained by AEMS function (in CYMA2DV code) which is calculated from “Gaunt factors” (Table 1 in [19]).

BII is obtained from AJI , BIJ is such that $\omega_i B_{ij} = \omega_j B_{ji}$, where ω_i is the statistical weight associated to level i .

Computation of collisional excitation rate coefficients (CECH function in CYMA2DV code):

Let n and n' be two levels ($n < n'$). The excitation rate coefficient is given by the following formula (Johnson, [19]), implemented in CYMA2DV code:

$$S_e(n, n') = (8kT/\pi m)^{1/2} \frac{2n^2}{x} \pi a_0^2 y^2 \left(A_{nn'} \left[\left(\frac{1}{y} + \frac{1}{2} \right) E_1(y) - \left(\frac{1}{z} + \frac{1}{2} \right) E_1(z) \right] \right) \\ + (8kT/\pi m)^{1/2} \frac{2n^2}{x} \pi a_0^2 y^2 \left(\left[B_{nn'} - A_{nn'} \ln \frac{2n^2}{x} \right] \left[\frac{1}{y} E_2(y) - \frac{1}{z} E_2(z) \right] \right) \quad (9.1)$$

$E_i(z) = \int_1^\infty e^{-zt} t^{-i} dt$ is called Exponential integral of order i ($i = 0, 1, 2, \dots$).

m denotes the electron mass and $a_0 = 0.5292 \cdot 10^{-8} \text{ cm}$ the Bohr radius.

Here and below, E_n denotes level energy of n for hydrogen. We obtain:

$$y = (E_{n'} - E_n)/kT, \\ z = r_{nn'} + y, \\ x = 1 - (n/n')^2, \\ B_{nn'} = \frac{4n^4}{n'^3} x^{-2} (1 + \frac{4}{3}x^{-1} + b_n x^{-2}), \\ b_n = n^{-1}(4 - 18.63n^{-1} + 36.24n^{-2} - 28.09n^{-3}), \quad n \geq 2, \\ A_{nn'} = 2n^2 x^{-1} f_{nn'}, \\ f_{nn'} = \frac{32}{3\sqrt{3}} \frac{n}{\pi n'^3} x^{-3} g(n, x), \\ g(n, x) = g_0(n) + g_1(n) x^{-1} + g_2(n) x^{-2}, \\ r_{nn'} = r_n x, \\ r_n = 1.94n^{-1.57}$$

where g_0, g_1, g_2 : Gaunt factors for pour Bound-Free transitions. They are given in Table 2 (Table 1 in [19]) :

Computation of collisional ionization rate coefficients (CICH function in CYMA2DV code):

	$n = 1$	$n = 2$	$n \geq 3$
$g_0(n)$	1.11330	1.0785	$0.9935 + 0.2328n^{-1} - 0.1296n^{-2}$
$g_1(n)$	-0.4059	-0.2319	$-n^{-1}(0.6282 - 0.5598n^{-1} + 0.5299n^{-2})$
$g_2(n)$	0.07014	0.02947	$n^{-2}(0.3887 - 1.181n^{-1} + 1.470n^{-2})$

Table 2: Gaunt factors

Let us consider here level n . Ionization rate coefficient is given by the following formula (Johnson, [19]) implemented in CYMA2DV code:

$$\begin{aligned}
S_i(n) = & (8kT/\pi m)^{1/2} 2n^2 \pi a_0^2 y_n^2 A_n \left[\frac{1}{y_n} E_1(y) - \frac{1}{z_n} E_1(z_n) \right] \\
& + (8kT/\pi m)^{1/2} 2n^2 \pi a_0^2 y_n^2 (B_n - A_n \ln 2n^2) [\zeta(y_n) - \zeta(z_n)],
\end{aligned} \tag{9.2}$$

where m is the electron mass and

$$\begin{aligned}
y_n &= I_n/kT, \\
z_n &= r_n + I_n/kT, \\
\zeta(t) &= E_0(t) - 2E_1(t) + E_2(t)
\end{aligned}$$

where I_n is ionization energy of level n for hydrogen.

Outputs: *AJI*, *BIJ*, *BJI*, *OIS*, *DLDFEF* in frequency and *DNDREF* in wavelength (Doppler width for Bound-Free transitions).

SOLINH

Definition of incident intensities for hydrogen lines in order to provide boundary conditions for the solution of radiative transfer equations.

The input file “intinc.dat” contains incident intensities for hydrogen lines. The input file “tembri.dat”, which is a table of brightness temperatures, is used to compute intensities *FINT* for the other hydrogen lines which are not in “intinc.dat”.

Inputs : *NN*, *NTT*, *NTAR*, *NFIMX*, *NCMX*, *NINF*, *NSUP*, *FRN*, *NTR*, *ICTR*, *NFINT*

Outputs : *FINT*, *CPOL*, *FRFI*

CIIM2

Computation of mean incident intensities HJMOY (integrating with respect to all directions), area by area, arriving on the cylinder and emitted from a sphere (Sun).

Inputs : *NCMX, RSOL, HAL, ALPHA, HIC, CPOL, PSI, NZETA, ZETA, NTHET, THETA, HJ1, HJ2*

Output : *HJMOY*

DEFCV

Definition of velocity fields (V_x, V_y, V_z). Many cases:

- static case: $V_x = V_y = V_z = 0$
- longitudinal flow of 30 km s^{-1} : $V_x = 0, V_y = 0, V_z = 3.10^6$
- rotation (0.01 rad s^{-1}): $V_{\text{max}} = 10 \text{ km s}^{-1}, V_z = 0, V_x \neq 0, V_y \neq 0$
- expansion ($V_{\text{max}} = 10 \text{ km s}^{-1}$): $V_z = 0, V_x \neq 0, V_y \neq 0$
- expansion ($V_{\text{max}} = 30 \text{ km s}^{-1}$): $V_z = 0, V_x \neq 0, V_y \neq 0$

EQST2D

Solution of statistical equilibrium: hydrogen level populations are computed by solving a linear system.

Inputs: *IOPMI, IVERB, NR, NPSI, NN, NTT, NTRD, NTRC, ITRD, ITRC, NINF, NSUP, CIJ, CJI, RIJ, RJI, RIC, RCI, HNT*

Output: *HN*

STYC2DV

Computation of intensity along the ray crossing the cylinder, knowing absorption coefficients (7.6), source functions (7.5) and intensities à each extremity of the cylinder.

STJC2DV

Equivalent to STYC2DV subroutine for continua.

DZTC2DV

Computation of the contribution to the diagonal of the Λ operator for the cylinder from Fourier components of the absorption coefficient. We build the tridiagonal system and we solve it.

TXCH2D

Computation of collisional transition probabilities (*CIJ* and *CJI*) using electron density.

Inputs: *NR, NPSI, NN, NTT, NTAB, NINF, NSUP, POM, FRN, TAB, OIS, TE, HNE*

Outputs: CIJ et CJI

MATIPS

Computation of interpolation matrices in Ψ (coordinate) since the points are not necessarily on a node of the grid or inside the grid.

10 Results for hydrogen lines in cylindrical threads

We consider a given model whose parameters vary inside the cylinder:

$PGMOD = 0.1 \text{ dyn cm}^{-2}$, $ALDEG = 0$, $HAL = 0 \text{ km}$, $R0KM = 500 \text{ km}$, $R1KM = 1000 \text{ km}$, $T0 = 6000 \text{ K}$, $T1 = 10^5 \text{ K}$, $TREF = 10^4 \text{ K}$.

The following figures for hydrogen lines are stored in the folder **results** when you download the package source file CYMA2DV.tgz from MEDOC website.

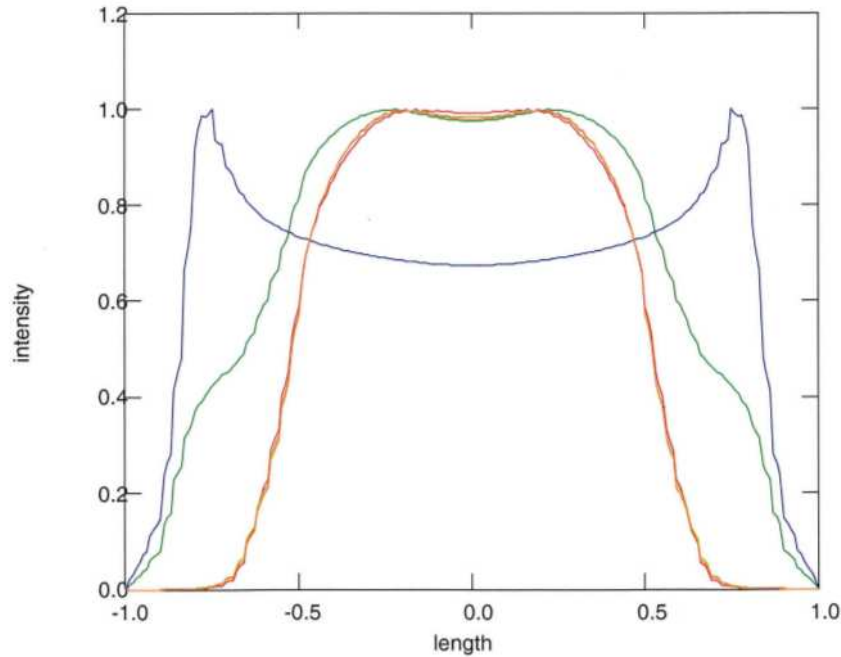


Figure 7: Relative intensities of $L\alpha$, $L\beta$, $H\alpha$ with respect to the position along an axis perpendicular to the cylinder

Figure 7 represents relative intensity for many hydrogen lines with respect to the position along an axis perpendicular to the cylinder. The blue curve represents relative intensity for

$L\alpha$, the green curve is relative intensity for $L\beta$, the red curve is relative intensity for $H\alpha$.

In figures 8, 9, 10, 11, 12, 13, relative wavelengths (\AA) are represented in abscissae ($\Delta\lambda$). In these figures, are also represented intensity variations across the bottom of the loop (vertical cylinder) for 10 equidistant positions (every 200 km) for intermediate radial velocity ($V_r = 30 \text{ km s}^{-1}$) for $L\alpha$, $L\beta$, $H\alpha$, $L\gamma$, $H\beta$, $Pa - \alpha$ lines. Each curve is shifted upwards with respect to the preceding one. The intensity scale for each graph is $\text{erg cm}^{-2} \text{ s}^{-1} \text{ sr}^{-1} \text{ \AA}^{-1}$.

In figures 14, 15, 16, 17, 18, 19, intensity variations across the bottom of the loop (vertical cylinder) for $L\alpha$, $L\beta$, $H\alpha$, $L\gamma$, $H\beta$, $Pa - \alpha$ lines are represented. Relative wavelengths (\AA) are in abscissae ($\Delta\lambda$) and distances in km are in ordinates.

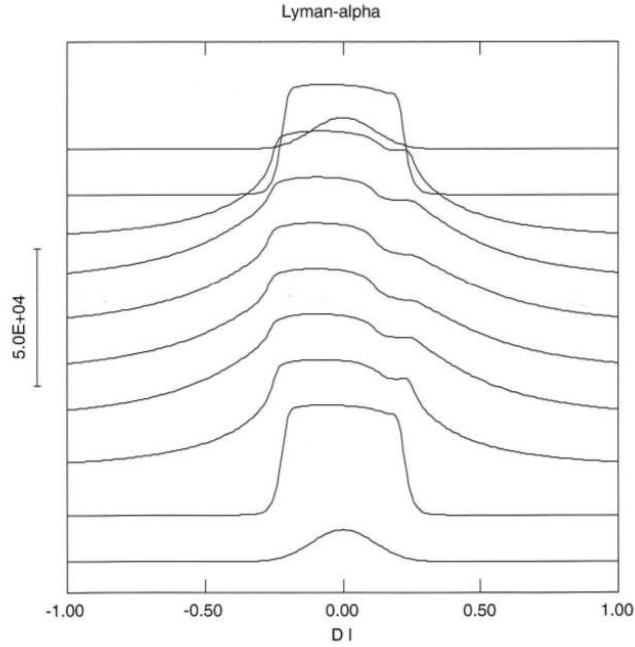


Figure 8: Intensity variations across the bottom of the loop for 10 equidistant positions (every 200 km) for $L\alpha$ line at 1215\AA . x-axis (\AA), y-axis ($\text{erg cm}^{-2} \text{ s}^{-1} \text{ sr}^{-1} \text{ \AA}^{-1}$)

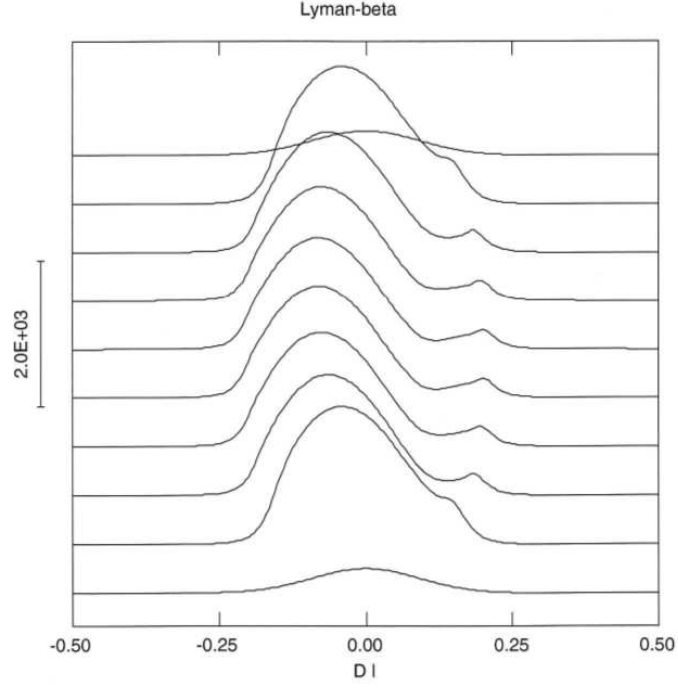


Figure 9: Intensity variations accross the bottom of the loop for $L\beta$ line at 1025\AA

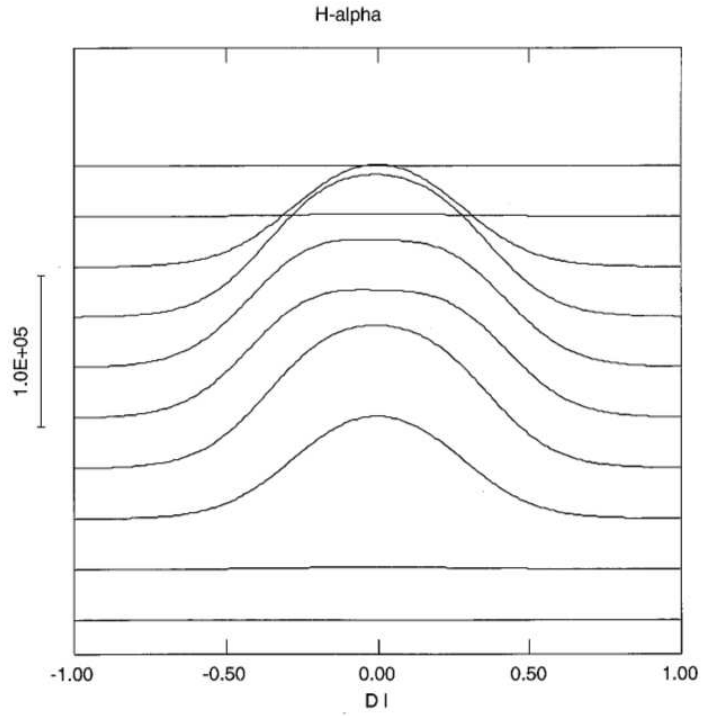


Figure 10: Intensity variations accross the bottom of the loop for $H\alpha$ at 6564\AA

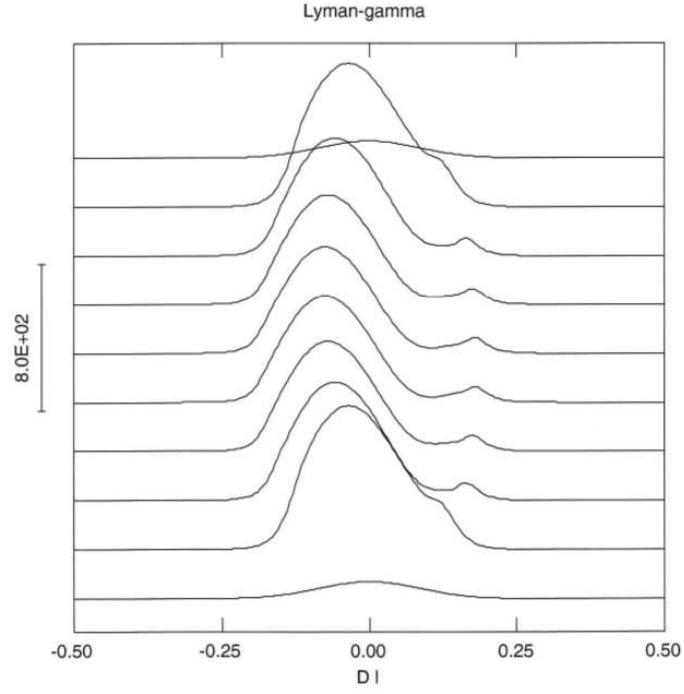


Figure 11: Intensity variations accross the bottom of the loop for $L\gamma$ at 972\AA

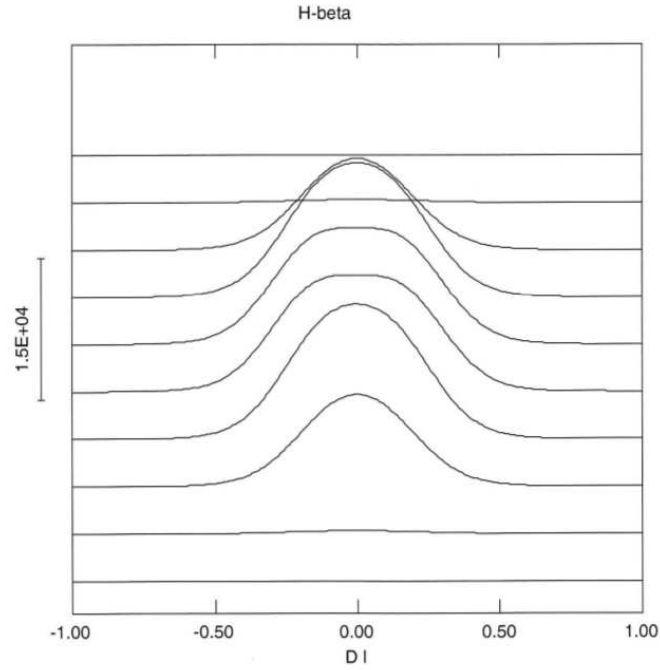


Figure 12: Intensity variations accross the bottom of the loop for $H\beta$ at 4862\AA

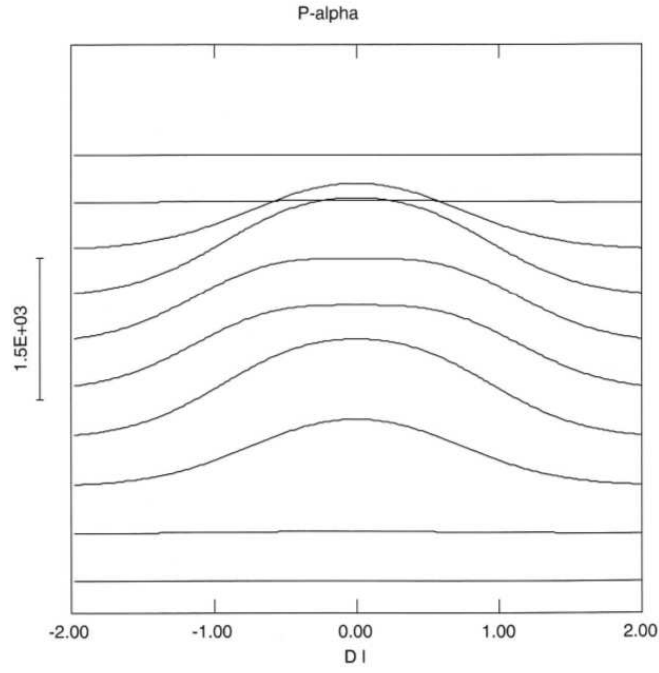


Figure 13: Intensity variations accross the bottom of the loop for $Pa - \alpha$ at 18756\AA

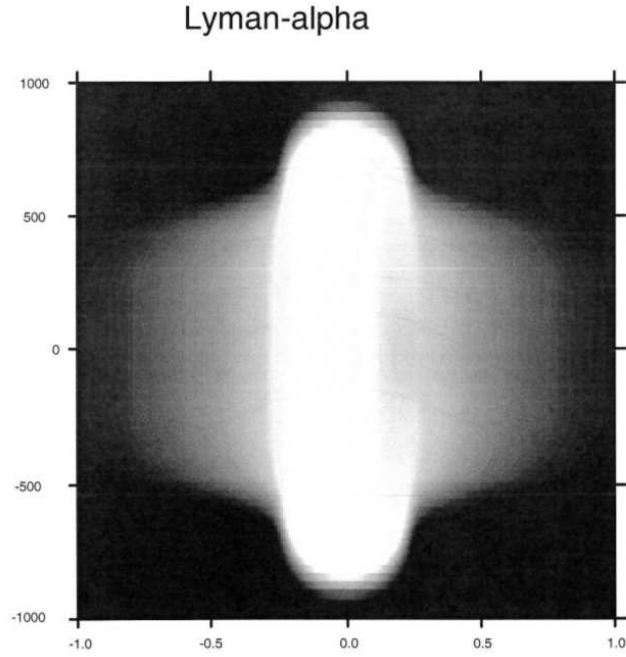


Figure 14: Intensity variations across the bottom of the loop for $L\alpha$ line at 1215\AA . Abscissae: relative wavelengths (\AA), Ordinates: distance in km

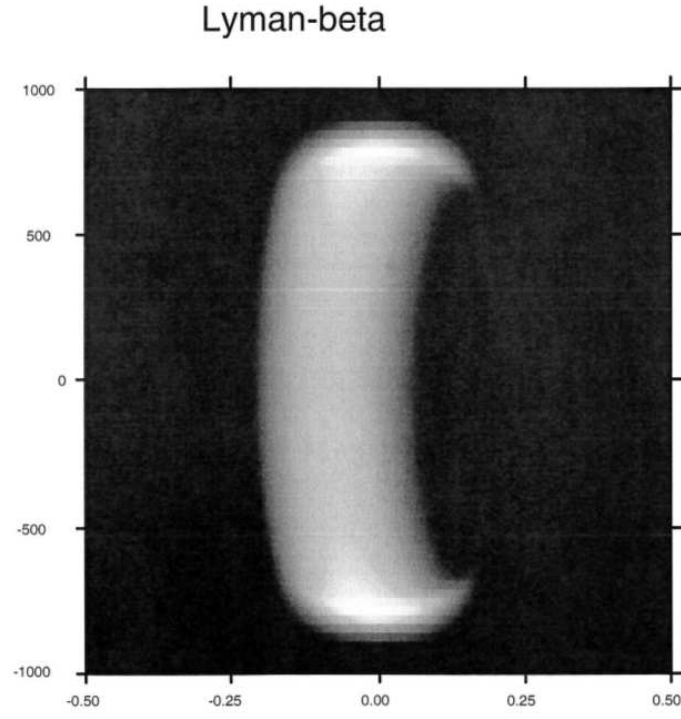


Figure 15: Intensity variations across the bottom of the loop for $L\beta$ at 1025\AA

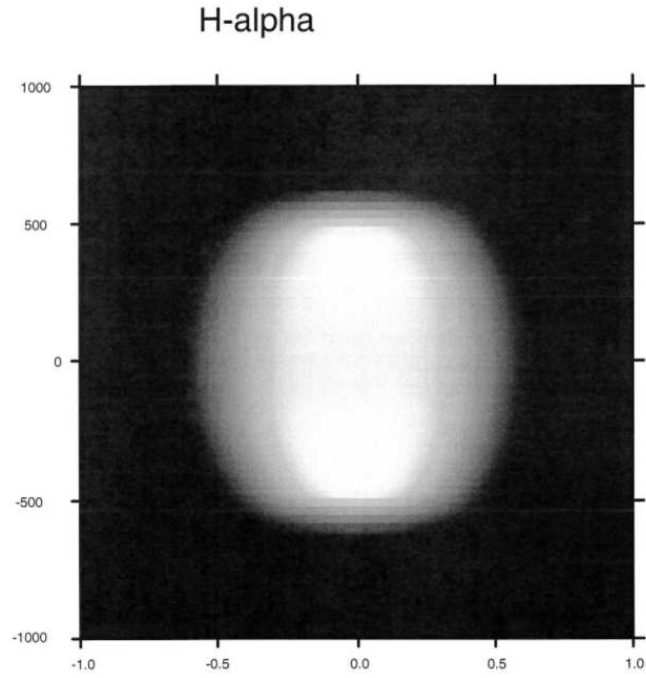


Figure 16: Intensity variations across the bottom of the loop for $H\alpha$ at 6564\AA

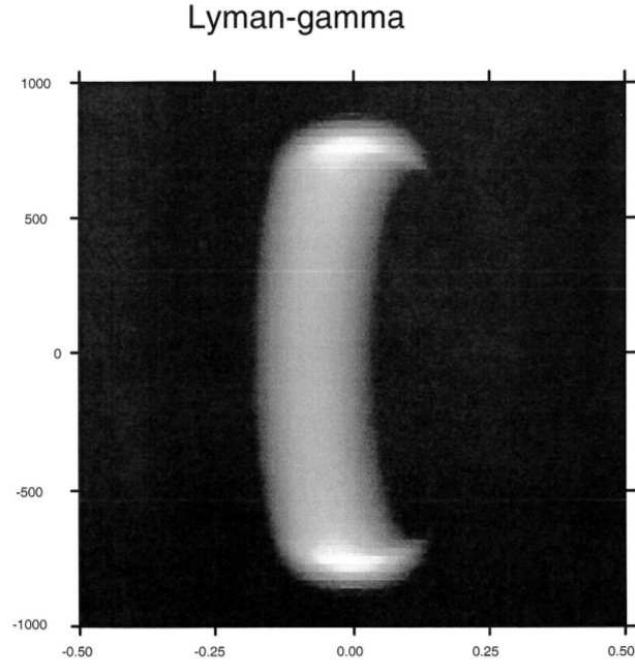


Figure 17: Intensity variations across the bottom of the loop for $L\gamma$ at 972\AA

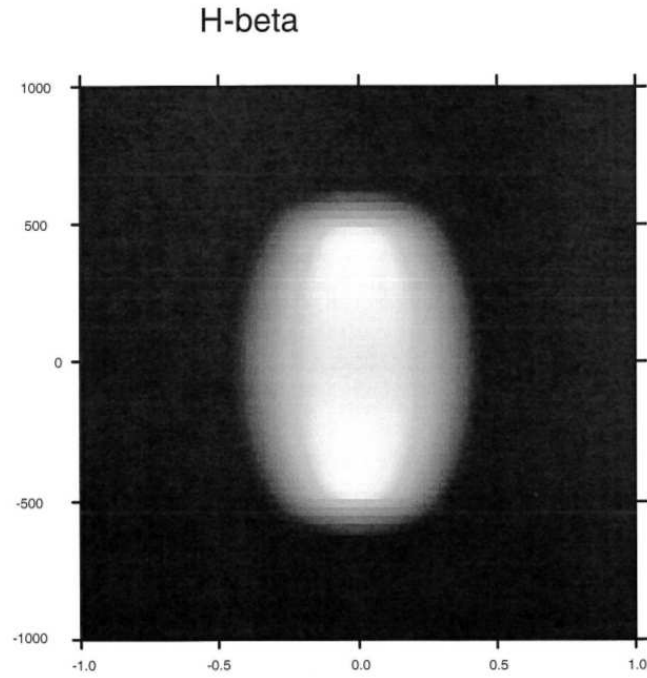


Figure 18: Intensity variations across the bottom of the loop for $H\beta$ at 4862\AA

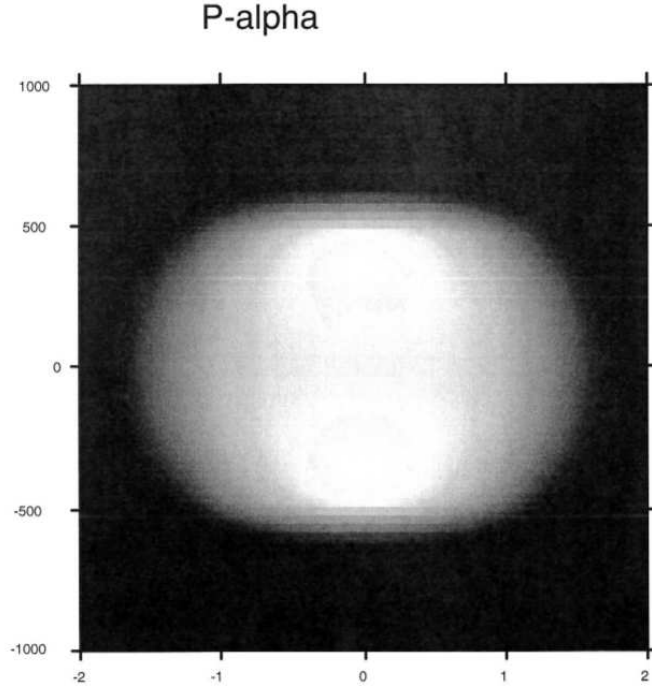


Figure 19: Intensity variations across the bottom of the loop for $Pa - \alpha$ at 18756\AA

11 Running CYMA2DV

- Download the package source file CYMA2DV.tgz from MEDOC website:
<https://idoc.osups.universite-paris-saclay.fr/medoc/tools/radiative-transfer-codes/>
- gfortran compiler is required.
- Unpack the package by typing the following linux command:
tar -xvzf CYMA2DV.tgz
- Go to folder CYMA2DV:
cd CYMA2DV
- The folder contains the following files: intinc.dat, tembri.dat, paramod.dat, makefile, cyma2dv.f90, visu.f90
- The file to modify is “paramod.dat”
- Run the code by typing:
make
./cyma2dv

- The output files are: cc2dhyv.log (iteration message), resu2dv.dat (emergent intensities for plotting line profiles), popc2dv.dat (hydrogen level populations), fort.8 (CPU time)
- The folder **results** contains the output files corresponding to a test case to be able to check if your results are good.
- To visualize results, use the following visualization program “visu.f90” :
`gfortran -o visu visu.f90`
`./visu`
 The output file is “cosbovi.ps”

12 CPU time

For a given model whose parameters vary inside the cylinder:

$\text{PGMOD} = 0.1 \text{ dyn cm}^{-2}$, $\text{ALDEG} = 0$, $\text{HAL} = 0 \text{ km}$, $\text{R0KM} = 500 \text{ km}$, $\text{R1KM} = 1000 \text{ km}$,
 $\text{T0} = 6000 \text{ K}$, $\text{T1} = 10^5 \text{ K}$, $\text{TREF} = 10^4 \text{ K}$.

On a PC with 4 Intel processors (2.67 GHz), the CPU time is 4719.213 s , i.e. 1h18.

13 Acknowledgements

We thank MEDOC directors: Eric Buchlin (present) and Frédéric Baudin (former).

31 October 2025

M. C-Y

References

- [1] C.W. Allen. *Astrophysical quantities*. The Athlone Press, University of London, 1973.
- [2] M. Arnaud and R. Rothenflug. An updated evaluation of recombination and ionization rates. *A&A suppl. Ser.*, 60:425–457, 1985.
- [3] L.H. Auer and D. Mihalas. On the use of variable Eddington factors in Non-LTE stellar atmospheres computations. *Mon. Not. R. astr. Soc.*, 149:65–74, 1970.
- [4] Eugene H. Avrett. *Introduction to Non-LTE radiative transfer and atmospheric modeling*. Lecture notes, 2008.
- [5] S. Chandrasekhar. *Radiative transfer*. Dover Publications, 1960.
- [6] CHIANTI Database. George Mason University (USA) and University of Michigan (USA) and University of Cambridge (UK). <http://www.chiantidatabase.org/>, Mai 2014.
- [7] K.P. Dere, E. Landi, H.E. Mason, B.C. Monsignori Fossi, and P.R. Young. CHIANTI - an atomic database for emission lines: I. Wavelengths greater than 50a. *A&A suppl. Ser.*, 125:149–173, 1997.
- [8] O. Gingerich. Review of Opacity Calculations. *Proceedings of the First Harvard-Smithsonian Conference on Stellar Atmospheres*, 167:1–25, 1964.
- [9] P. Gouttebroze. Radiative transfer in cylindrical threads with incident radiation. *A&A*, 413:733–743, 2004.
- [10] P. Gouttebroze. Radiative transfer in cylindrical threads with incident radiation. II : 2D azimuth-dependent case. *A&A*, 434:1165–1171, 2005.
- [11] P. Gouttebroze. Radiative transfer in cylindrical threads with incident radiation. III : Hydrogen spectrum. *A&A*, 448:367–374, 2006.
- [12] P. Gouttebroze. Radiative transfer in cylindrical threads with incident radiation. V : 2D transfer with 3D velocity fields. *A&A*, 487:805–813, 2008.
- [13] P. Gouttebroze, P. Heinzel, and J.-C. Vial. The hydrogen spectrum of model prominences. *A&A Suppl. Ser.*, 99:513–543, 1993.
- [14] P. Gouttebroze and N. Labrosse. A ready-made code for the computation of prominence NLTE models. *Solar Physics*, 196:349–355, 2000.
- [15] P. Gouttebroze and N. Labrosse. Radiative transfer in cylindrical threads with incident radiation. VI : A hydrogen plus helium system. *A&A*, 503:663–671, 2009.
- [16] Pierre Gouttebroze. *Formation des raies spectrales et oscillations dans la chromosphère solaire*. Thèse d’Etat, Université Paris 7, 1980.

- [17] I. Hubeny and D. Mihalas. *Theory of Stellar Atmospheres : An introduction to Astrophysical Non-equilibrium Quantitative Spectroscopic Analysis*. Princeton University Press, 2015.
- [18] J.T. Jefferies. *Spectral line formation*. Blaisdell, 1968.
- [19] L.C. Johnson. Approximation for collisional and radiative transition rates in atomic hydrogen. *A&A*, 174:227–236, 1972.
- [20] Nicolas Labrosse. *Modélisation du spectre de l’hélium dans les protubérances solaires*. PhD thesis, Université Paris XI Orsay, 2001.
- [21] P. Lemaire, P. Gouttebroze, J.-C. Vial, and G. E. Artzner. Physical properties of the solar chromosphere deduced from optically thick lines: I. Observations, data reduction, and modelling of an average plage. *A&A*, 103:160–176, 1981.
- [22] G. L. Olson, L. H. Auer, and J. R. Buchler. A rapidly convergent iterative solution of the non-lte line radiation transfer problem. *JQSRT*, 35, 431:733–743, 1986.
- [23] J. Oxenius. *Kinetic Theory of Particles and Photons. Theoretical Foundations of Non-LTE Plasma Spectroscopy*. Springer-Verlag, 1986.
- [24] F. Paletou. Transfert de rayonnement : méthodes itératives. *C. R. Acad. Sci. Paris*, t. 2, Série IV:885–898, 2001.
- [25] G. Peach. A general formula for the calculation of absorption cross sections for free-free transitions in the field of positive ions. *Royal Astronomical Society*, 130:361–377, 1964.
- [26] C. Pecker-Wimel. *Introduction à la spectroscopie des plasmas*. Gordon and Breach, 1966.
- [27] R.J. Rutten. *Radiative transfer in stellar atmospheres*. 2003.
- [28] E. Schatzman. *Astrophysique*. Masson et Cie, 1963.
- [29] J.E. Vernazza, E. H. Avrett, and R. Loeser. Structure of the Solar chromosphere; ii. The underlying photosphere and temperature-minimum region. *ApJS*, 30:1–60, 1976.